Non-linear vibration signal compensation technique for UAV-deployable sensor packages with edge computing

Joud N. Satme[a], Daniel Coble[a], Hung-Tien Huang[b], Austin R.J. Downey[a,c], and Jason D. Bakos[b]

[a]Department of Mechanical Engineering, University of South Carolina, Columbia, SC, USA 29201

[b]Department of Computer Science and Engineering, University of South Carolina, Columbia, SC, USA 29201

[c]Department of Civil and Environmental Engineering, University of South Carolina, Columbia, SC, USA 29201

ABSTRACT

For rapid assessment of infrastructure, the use of minimally invasive sensors that can be deployed remotely using autonomous vehicles is gaining popularity. Such systems are favorable for their ease of deployment and cost-effectiveness. Utilizing electropermanent magnets or adhesives to mount the sensors temporarily forms a barrier between the sensor and the structure being examined. This barrier creates undesirable nonlinearities and transmissibility losses that introduce errors into structural damage detection algorithms. Post-processing of signals using continuous modeling techniques from classical control theory can be applied to the collected signals to remove this error. However, post-processing creates additional analysis steps that require the signal to be taken off device. Processing the data at-the-edge prior to saving it to memory or transmitting it to a base station enables rapid assessment of infrastructure. With minimal time from signal detection to prognostics, such systems can be used in damage forecasting and infrastructure failure prevention. This preliminary work aims to develop a non-linear machine-based compensation technique that is resource and power efficient enough to be processed on-device. The proposed long short-term memory (LSTM) error-compensating network demonstrated potential by increasing the SNR_{dB} by 9.3% and improving RMSE by approximately 20% while widening the usable lower limit of the sensor's bandwidth from 2.78 to 1.34 Hz. The progress described in this report focuses on setting the framework for the proposed method and paves the way for a full-scale hardware implementation in the near future.

Keywords: edge-computing sensor package, UAV-deployable sensor systems, rapid structural health monitoring, LSTM error compensation network, vibration-sensing node, neural network filter, minimal invasiveness sensor, standalone sensing systems

1. INTRODUCTION

Wireless sensing networks have proven to be useful tools for structural health monitoring (SHM). Due to their compact footprint and ease of deployment, such networks are ideal for rapid structural assessment applications.[1] Wireless sensing networks have been widely used in the monitoring of civil structures utilizing vibration-based modal analysis algorithms.[2] Of particular interest to this work is the ability to deploy such wireless networks onto currently operational or historic structures while minimizing environmental or cultural concerns.[3]

Unmanned aerial vehicles (UAV) are increasingly being used to deploy wireless sensor nodes for SHM applications. UAV-deployable wireless sensor networks enable the diagnostic process of a structure to be streamlined, eliminating the need for personnel to be in danger zones of traffic or unstable structures. In addition, these systems are advantageous in that a small number of sensing nodes can be rapidly mobilized and re-positioned along a structure,[4] for instance, in experimental modal analysis applications of suspended bridges.[5] As a result of their

Further author information: (Send correspondence to Austin R.J. Downey)
Austin R.J. Downey: E-mail: austindowney@sc.edu

Sensors and Smart Structures Technologies for Civil, Mechanical, and Aerospace Systems 2023, edited by Zhongqing Su, Branko Glisic, Maria Pina Limongelli, Proc. of SPIE Vol. 12486, 124861M · © 2023 SPIE · 0277-786X · doi: 10.1117/12.2658563

desirable characteristics, such networks have shown promise as reliable, low-cost alternatives to hard-wired SHM sensing systems. UAV-deployable wireless sensor nodes and networks have been studied for SHM applications including [6–9].

A shortcoming of minimally invasive sensors is the mounting medium that maintains contact between the actual vibration sensor and the structure of interest. Magnets and adhesives have been used to varying degrees of success,[10–12] with transmissibility loss being the main limitation.[13,14] When vibration propagates through the contact medium, some of the signal strength is lost through the magnet/metal interface and the natural damping of the material. This damping property can have a major negative impact when the vibration signal is low-energy. Typically, civil infrastructure vibration signatures tend to be at lower frequencies (< 100 Hz) with acceleration amplitudes in the mg-μg scale, where any transmissibility loss can cause the signal to degrade below the resolution of the accelerometer on board the sensor package.[15] This loss has the greatest impact on SHM algorithms that use ambient vibration rather than an excitation source.[16] Although traditional control approaches have shown some promise in increasing the signal-to-noise ratio and mitigating transmissibility loss via filter transfer functions,[17,18] the low-energy low-frequency scale remains a difficult range to address because the sensor's nonlinearity is prominent within that bandwidth, specifically 0-5 Hz.

To address the transmissibility challenge in UAV-deployed sensor packages, a nonlinear deep-learning approach based on a long short-term memory (LSTM) developed to run on board a UAV-deployable sensor package is investigated. The proposed method demonstrated flexibility during model training, and the ability to tackle complex sensor non-linearity in the low-frequency scale (< 5 Hz), as well as improving signal quality on-edge, eliminating post-processing steps, all of which are desirable characteristics for rapid SHM applications. The contributions of this work are on two fronts. First, a report on the process of constructing training and testing datasets through an experimental approach, training a neural network error-compensating model, and finally assessing the model's ability to mitigate transmissibility loss through measurable metrics is reported. Second, an investigation is conducted into the feasibility of deploying such models on limited-performance computers and embedded systems utilized in minimal invasiveness sensors for SHM applications.

2. BACKGROUND

This section reports on the required background elements of this paper.

2.1 Open-source UAV-deployable vibration sensor

The authors have developed an open-source UAV-deployable vibration sensor for SHM applications as shown in Figure 1. The sensor package consists of an electropermanent magnet[19] for attaching the sensor package to steel structures, a capacitive micro-electro-mechanical system (MEMS)-based accelerometer, and a microcontroller to handle the sensor node's data acquisition and control.[4] A network of these sensor packages has been previously tested in an experimental modal analysis framework.[20]

The sensor package utilized in the model training phase of this work consists of the Teensy 4.0 microcontroller with its ARM Cortex-M7 microprocessor. The package also features an independent power system comprising of a 2-cell lithium polymer battery and a power regulation and conditioning module. Non-volatile memory is chosen to store data on board, due to its desired footprint and low power consumption. An SCA-3300-d01 MEMS accelerometer was embedded into the frame of the EPM V3R5C electropermanent magnet to establish contact with the structure, a design choice made with minimizing transmissibility loss in mind. An NRF24L01 wireless module operating on the 2.4 GHz enhanced ShockBurst protocol is also included. This feature enables the sensor package to receive control commands, communicate with other sensor packages, or send data and status updates to a base station. The hardware utilizes the Serial Peripheral Interface (SPI) as its wired communication protocol for its favorable speed. This is required for sensor-memory interface and data transfer processes. With aerial deployment in mind, a lightweight 3D printed PLA frame was designed to house the delicate electronics and shield them from the environment during field deployments; yet still be compact and light for UAV delivery. This sensor package framework and all related designs have been made available as an open-source project.[21]

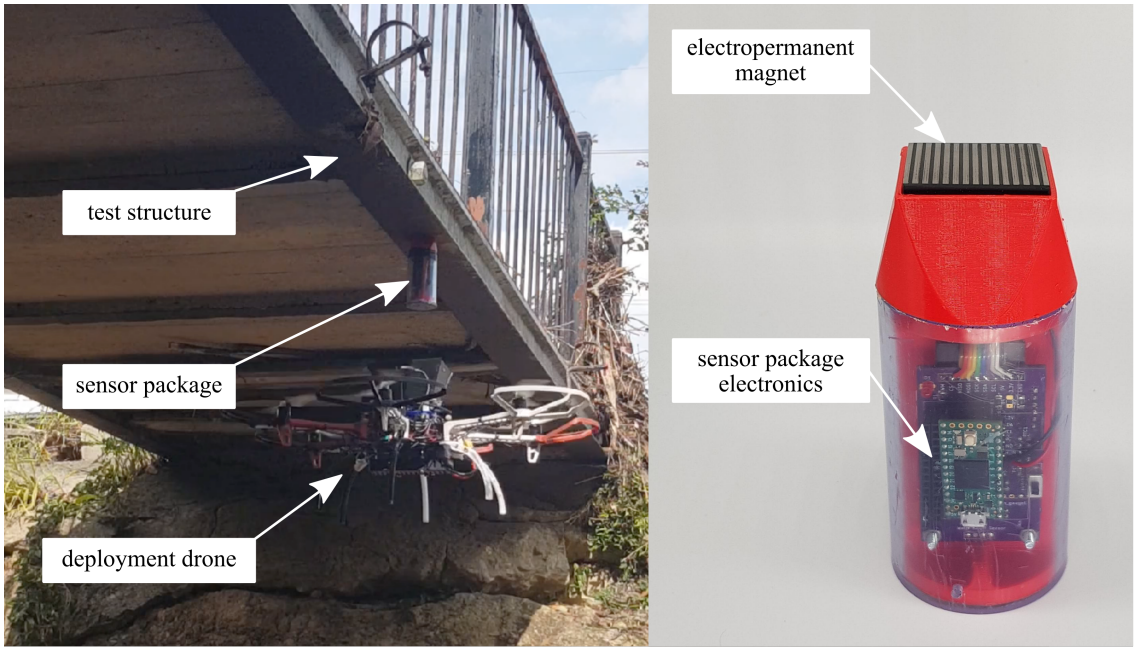

Figure 1. (a) Sensor package deployment under a pedestrian bridge, (b) sensor package and electropermanent magnet configuration.

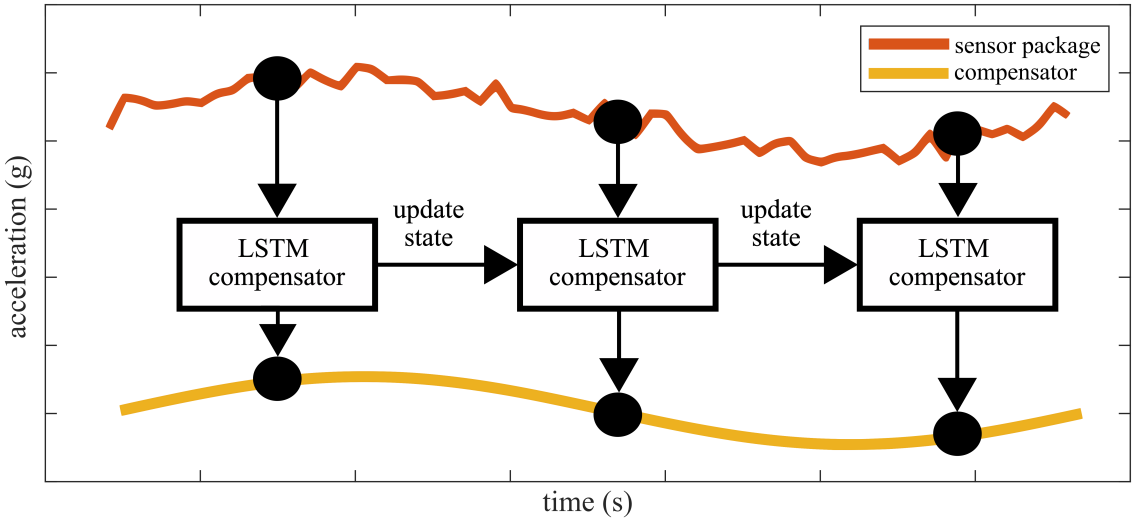

Figure 2. Edge implementation of the LSTM compensator network for signal conditioning.

2.2 LONG SHORT-TERM MEMORY NETWORKS

Long short-term memory (LSTM) are a class of deep-learning artificial neural networks for processing time-series data. The principle of the LSTM network, as it is with any recurrent neural network (RNN), is to use a feedback connection to pass state information to future timesteps. The state information allows an LSTM model to make predictions based on all previous data in the time series. Their ability to predict based on temporal patterns makes them ideal for processing vibration data; as done in this work. In an LSTM model set up for signal

compensation, a data point enters the model as a singleton vector x_t. The LSTM forward pass updates the internal state vectors h_t and c_t and returns the updated h_t vector. The size of the vectors h_t and c_t is termed the units of the model, and it is generally expected that models with more units are capable of processing more complex signals. As the desired output is a single datapoint, a dense layer takes the output of the LSTM and produces a singleton output by means of a vector inner product with the weights and bias add, a process simplified as shown in Figure 2. The seven driving equations of the model are presented in equations 1-7, with equations 1-6 describing the LSTM forward pass and equation 7 describing the dense layer.[22,23] Nonlinearity is provided by the σ and tanh activation functions.

$$f_t = \sigma(W_f x_t + U_f h_{t-1} + b_f) \tag{1}$$
$$i_t = \sigma(W_i x_t + U_i h_{t-1} + b_i) \tag{2}$$
$$o_t = \sigma(W_o x_t + U_o h_{t-1} + b_o) \tag{3}$$
$$\tilde{c}_t = \tanh(W_c x_t + U_c h_{t-1} + b_c) \tag{4}$$
$$c_t = f_t \circ c_{t-1} + i_t \circ \tilde{c}_t \tag{5}$$
$$h_t = o_t \circ \tanh(c_t) \tag{6}$$
$$y_t = W_d^T h_t + b_d \tag{7}$$

3. METHODOLOGY

This section presents the LSTM compensator model in addition to the sensor package hardware breakdown and the experimental testing procedure.

3.1 LSTM-BASED COMPENSATOR MODEL

Temporal noise rejection and error-compensating models can take many forms with their similarity being the recognition of undesirable or false sensor measurements. Undesirable sensor anomalies can be categorized into two main types: phase error, defined as the time lag between the temporal event occurring and its detection by the sensor, and magnitude related error, which is classified as the under or overcompensation of the measurement's gain. Authors of this work have previously investigated a controls-based approach by developing a continuous transfer function model that corrected the gain-related error using an input-output relationship between a superior reference accelerometer and a lower performance accelerometer utilized in low-cost sensor packages.[18] This approach has shown potential in enhancing the signal's quality with some notable limitations. The model lacked the adequate generalization and was only fitted to one type of excitation signals. The model was also heavily reliant on the training data as minor changes in phase between the input and output signals impacted the model performance significantly. This was attributed to high non-linearity that a linear transfer function could not account for. LSTM-based compensator models tackle such challenges by being nonlinear systems themselves. This feature enables the network to recognize complex sensor anomalies and reject them from the measurement. LSTM networks are also more adaptable in terms of architecture and training procedure, allowing batches of different tests with different excitation signals to be fed into the network for a more generalized model. When compared to transfer function filters, one drawback of LSTM error-compensating models is their high computational load and large memory footprint. These characteristics make deploying such networks on low-performance computers a difficult task, requiring design trade-offs be made between performance and model size for a successful deployment.

3.2 EXPERIMENTAL TRAINING AND VALIDATION

To develop the LSTM compensation model, data across the bandwidth of interest is needed. An experimental setup is built in order to provide training data to the compensator model. The setup, shown in Figure 5 (a), includes an electromagnetic shaker as the mechanical excitation source, the sensor package, along with a superior reference accelerometer as the ground truth measurement. A signal generation and data acquisition system is also used to generate the excitation signal through an analog output module, start both sensors simultaneously

using a digital trigger, and finally, an analog input module is included to record the reference accelerometer signal.

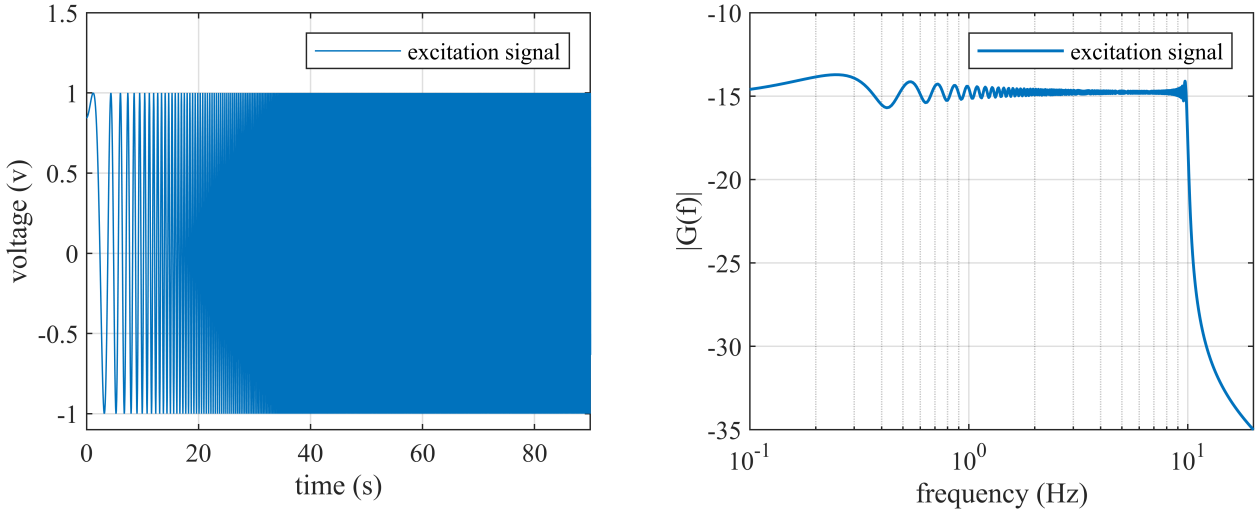

Figure 3. Normalized Chirp excitation signal: (a) time domain, and; (b) frequency domain plots.

The chosen excitation signal was a frequency sweep also known as Chirp excitation. The model performed better during training when only one frequency was presented at a time, thus the choice of the excitation signal. The Chirp waveform, shown in Figure 3, was created initially with the mathematical formula

$$x(t) = \sin\left(2\pi\left(\frac{f_{\text{end}} - f_{\text{start}}}{2(\text{test time})}t^2 + f_{\text{start}}t\right)\right) \tag{8}$$

A voltage signal is then synthesized and fed into the electromagnetic shaker through a power amplifier. The datasets were of 74000 samples taken at a sampling frequency of 400 S/s. The model was provided with training frequency sweeps within the range of 0-10 Hz with various dynamic ranges to further enhance its performance.

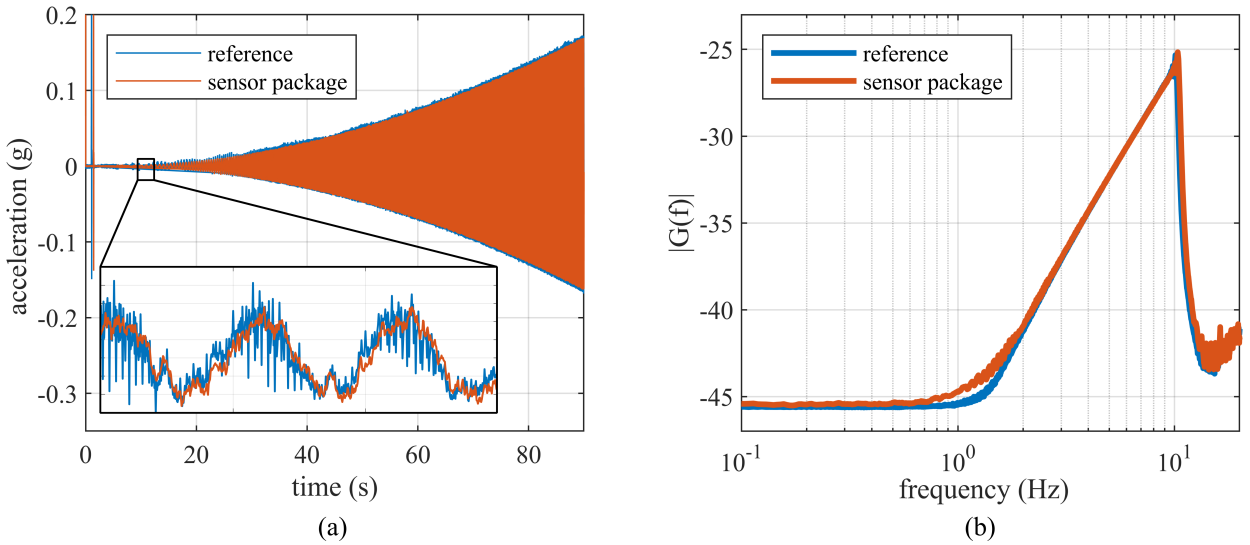

Figure 4. One of the training datasets in the range of 0 - 10 Hz: (a) time domain, and; (b) frequency domain plots.

A primary investigation during the training dataset construction revealed a large deviation in measurement within the low-frequency scale (< 5 Hz). The decision was made to expand the training scope to 0-10 Hz because

the error-compensating model required data from a wide dynamic range to refine its prediction quality. Figure 4 shows that increasing the frequency is directly proportional to increasing the magnitude of actuation, thereby expanding the dynamic range over which the model can train. Although increasing the bandwidth of training data resulted in a significant overall improvement, the 0-5 Hz scale remained the focus during the experimental phase.

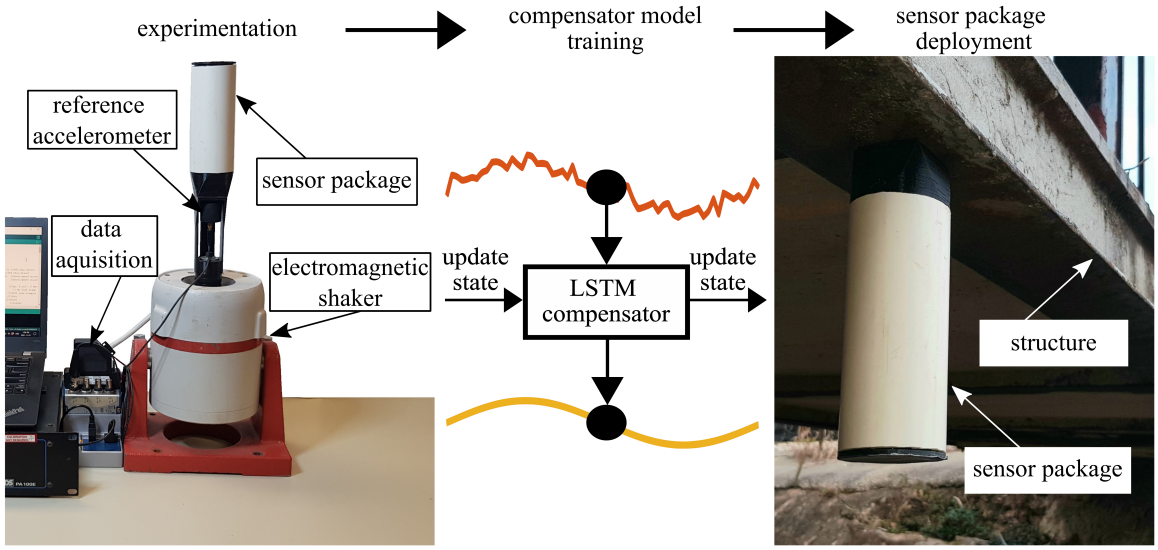

Figure 5. Flow chart of (a) experimental setup for developing training data, (b) edge implementation of the LSTM compensator, and; (c) sensor field deployment on a pedestrian bridge.

To ensure a successful training process where the focus was training on the dynamic range of the signal, an assumption of zero phase between the two sensors was made. Because the sensor package and data acquisition were running on different clocks, an impulse was fed through the shaker prior to each test iteration so that the samples could be precisely aligned after the experiment. The reference accelerometer of choice was a Integrated Electronics Piezoelectric sensor (IEPE), which performed considerably better than the low-cost Micro Electromechanical Systems (MEMS) accelerometer on board the sensor package. The purpose of this experiment was to generate a supervised learning dataset to train an error-compensating model that will be deployed onto sensor packages in the field as shown in Figure 5 (b).

3.3 COMPENSATOR MODEL TRAINING

The training dataset consisted of six frequency sweeps: 0-1, 1-2, 2-3, 3-4, 4-5, and 0-10 Hz, shown in Figure 4. Each training experiment was 90 s in length and sampled at 400 S/s. By including more data from the 0-5 Hz region, the training dataset emphasized improvement in the lower hertz range. Furthermore, an additional 90 s dataset for testing in the range of 0-5 Hz was used. The testing dataset was run independently, so no data was shared between training and testing. In other words, while the testing dataset will be similar to a training frequency sweep, it will not share the specific noise profile that the LSTM model is expected to compensate for.

Model training was performed using the tensorflow.keras module. The chosen model consists of a single LSTM layer of 50 units. A dense layer converts the 50-element vector output of the LSTM to the output acceleration prediction. Training utilized the Adam optimizing algorithm with a learning rate of 0.001, β_1 of 0.9, β_2 of 0.999, and ϵ of 1e-07. During training, the model was observed to converge to a satisfactory level in 30 epochs. Preliminary investigations into model architecture revealed that the model size could be reduced without significant loss in performance, however as the chosen model performed well within the execution time and memory constraints without the need for additional compromise, minimal model size was not investigated further in this work.

Training followed an online scheme, where each frequency sweep dataset was fed in its entirety to the LSTM, with backpropagation and weight updating performed every 400 samples (equivalent to one second of signal prediction). To gauge the LSTM compensator network's performance, equations 9 and 10 were used to calculate $\mathrm{SNR_{dB}}$ and RMSE respectively.

$$\mathrm{SNR_{dB}} = 10\log_{10}\left(\frac{\sum_{i=1}^{\text{data length}}(\text{signal}(i))^2}{\sum_{i=1}^{\text{data length}}(\text{noise}(i))^2}\right) \tag{9}$$

$$\mathrm{RMSE} = \sqrt{\frac{\sum_{i=1}^{\text{data length}}(\text{truth(i)} - \text{prediction(i)})^2}{\text{data length}}} \tag{10}$$

4. RESULTS AND DISCUSSION

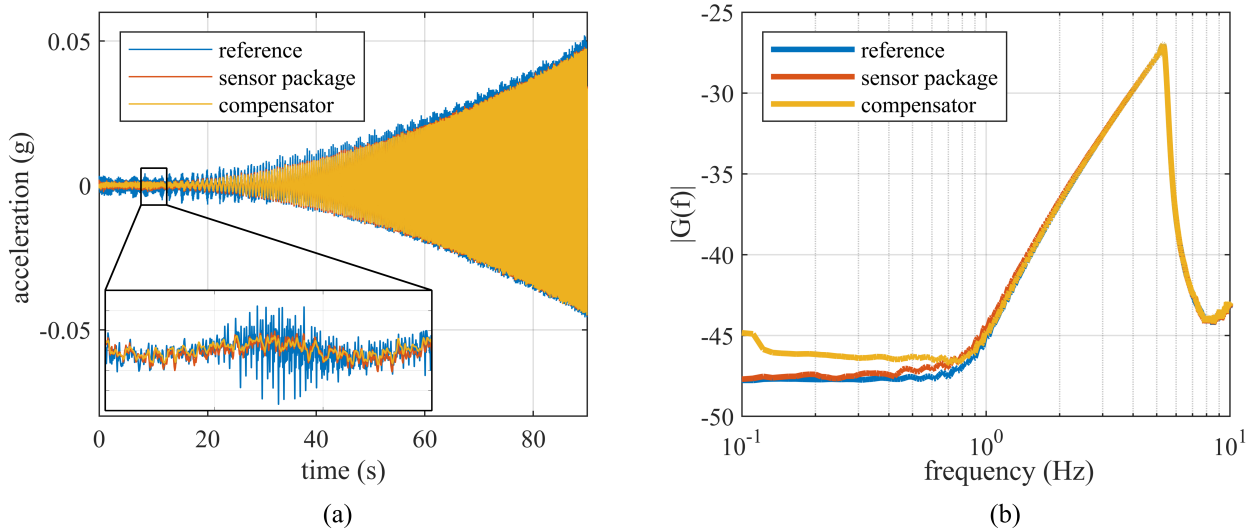

Figure 6. A comparison of performance between the sensor package and the compensator network, showing: (a) time domain, and; (b) frequency domain plots utilizing the testing dataset.

To examine the compensator network prediction quality, a testing dataset is fed into the model in the bandwidth of interest (0-10 Hz). The compensator network is shown to trace the reference accelerometer sufficiently well in the range of 1-10 Hz. An increase in gain in the lower frequency scale (< 0.9 Hz) is shown in Figure 6 (b). This anomaly can be attributed to the training dataset bias towards the lower bandwidth or the lack of adequate resolution in the ± 3 mg dynamic range leading to a degradation in prediction quality.

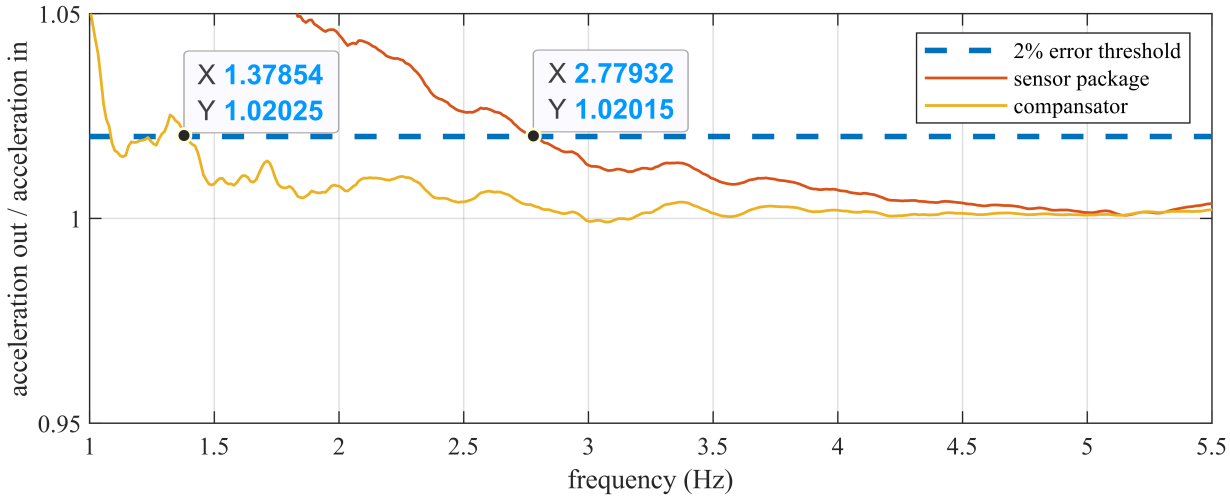

Figure 7. Frequency response function of the sensor package and the compensator network in the range of 0-5 Hz.

Figure 7 reports the expansion in usable bandwidth of the sensor package. A Frequency response function was used to represent the improvement in the lower frequencies. A 2% error threshold was set, and as illustrated in Figure 7, the compensator was able to maintain an error lower than the threshold as low as 1.379 Hz in comparison to the raw sensor that surpassed that threshold at 2.779 Hz, producing a 1.4 Hz expansion in usable bandwidth. Further improvement is reported in Table 1 where the LSTM compensator achieved a $\mathrm{SNR_{dB}}$ of 18.88 dB a 9.34% enhancement. Additionally, a significant improvement in error rejection was demonstrated, with the network achieving an RMSE of 1.44×10^{-3} g, a 19.66% decrease from the raw sensor signal.

Table 1. A comparison between the raw sensor measurements and the compensated signal using signal-to-noise ratio and RMSE in the bandwidth of 0-10 Hz.

testing	$\mathrm{SNR_{dB}}$	RMSE
sensor package	17.26 dB	1.795×10^{-3}
LSTM compensator	18.88 dB	1.442×10^{-3}
% improvement	9.34%	19.66%

To assess the viability of hardware implementation, the trained LSTM model is serialized to open neural network exchange (ONNX) to then be deployed onto a Raspberry Pi 4 with 2 GB of RAM, running Ubuntu Mate 20.04. The model was deployed in 32-bit precision, consuming 5.1 MB of memory. In a forward pass over the testing dataset, the model-averaged 10 μs per prediction, resulting in a forward pass execution frequency of 100 kS/s, well over the 400 S/s threshold set by the SHM sensor sampling rate. The runtime memory consumption was measured at 36.8 MB as reported by the profiler. All model parameters were well within the thresholds set by the intended SHM application.

5. CONCLUSION

In applications requiring rapid assessment of structures, high-mobility minimal invasive sensors have demonstrated great potential. Low cost, small footprint, and ease of deployment distinguish such systems from their hardwired counterparts. This work presents a framework to further enhance the performance of minimal invasiveness sensors by overcoming the transmissibility loss caused by the mounting medium. To overcome this

challenge an online LSTM compensator was proposed, with the focus of the study being the signal quality enhancement of the accelerometer on board the sensor package, as well as the feasibility of deploying such models on-edge. Results show an enhancement of 9.3% in SNR_{dB} and an RMSE decrease of 20% in addition to frequency response function analysis that indicated an expansion of 1.4 Hz in the usable sensor bandwidth (<2% error). These results demonstrate that an LSTM error-compensating network is a viable approach to reduce signal degradation attributed to transmissibility loss. Future work will concentrate on improving the network performance in the lower frequencies while also minimizing model size to reduce computational load, thereby paving the way for an embedded system implementation.

ACKNOWLEDGMENTS

This material is based upon work supported by the Air Force Office of Scientific Research (AFOSR) through award no. FA9550-21-1-0083. This work is also partly supported by the National Science Foundation Grant numbers 1937535, 1956071, 2152896, and 2237696.

REFERENCES

[1] Noel, A. B., Abdaoui, A., Elfouly, T., Ahmed, M. H., Badawy, A., and Shehata, M. S., "Structural health monitoring using wireless sensor networks: A comprehensive survey," *IEEE Communications Surveys & Tutorials* **19**(3), 1403–1423 (2017).

[2] Bernardini, L., Benedetti, L., Somaschini, C., Cazzulani, G., and Belloli, M., "SHM campaign on 138 spans of railway viaducts by means of OMA and wireless sensors network," in [*Lecture Notes in Civil Engineering*], 15–25, Springer International Publishing (aug 2022).

[3] Ierimonti, L., Cavalagli, N., Venanzi, I., García-Macías, E., and Ubertini, F., "A bayesian-based inspection-monitoring data fusion approach for historical buildings and its post-earthquake application to a monumental masonry palace," *Bulletin of Earthquake Engineering* **21**, 1139–1172 (Dec. 2022).

[4] Carroll, S., Satme, J., Alkharusi, S., Vitzilaios, N., Downey, A., and Rizos, D., "Drone-based vibration monitoring and assessment of structures," *Applied Sciences* **11**(18) (2021).

[5] Zhou, H., Lynch, J., and Zekkos, D., "Autonomous wireless sensor deployment with unmanned aerial vehicles for structural health monitoring applications," *Structural Control and Health Monitoring* **29** (mar 2022).

[6] Sreenath, S., Malik, H., Husnu, N., and Kalaichelavan, K., "Assessment and use of unmanned aerial vehicle for civil structural health monitoring," *Procedia Computer Science* **170**, 656–663 (2020). The 11th International Conference on Ambient Systems, Networks and Technologies (ANT) / The 3rd International Conference on Emerging Data and Industry 4.0 (EDI40) / Affiliated Workshops.

[7] Whelan, M. J., Gangone, M. V., Janoyan, K. D., and Jha, R., "Real-time wireless vibration monitoring for operational modal analysis of an integral abutment highway bridge," *Engineering Structures* **31**(10), 2224–2235 (2009).

[8] Krishnamurthy, V., Fowler, K., and Sazonov, E., "The effect of time synchronization of wireless sensors on the modal analysis of structures," *Smart Mater. Struct.* **17**, 055018 (Oct. 2008).

[9] Bocca, M., Eriksson, L. M., Mahmood, A., Jäntti, R., and Kullaa, J., "A synchronized wireless sensor network for experimental modal analysis in structural health monitoring," *Computer-Aided Civil and Infrastructure Engineering* **26**(7), 483–499 (2011).

[10] Takeuchi, K., Masuda, A., Akahori, S., Higashi, Y., and Miura, N., "A close inspection and vibration sensing aerial robot for steel structures with an epm-based landing device," 101692U (04 2017).

[11] Takeuchi, K., Masuda, A., Akahori, S., Higashi, Y., and Miura, N., "An aerial robot landing on a steel structure for vibration measurement: -elimination of an influence of airframe vibration-," *The Proceedings of the Symposium on Evaluation and Diagnosis* **2016.15**, 209 (01 2016).

[12] Boehme, B., Roellig, M., and Wolter, K.-J., "Moisture induced change of the viscoelastic material properties of adhesives for shm sensor applications," in [*2010 Proceedings 60th Electronic Components and Technology Conference (ECTC)*], 1885–1892 (2010).

[13] Liu, X., Xu, Y., Wang, X., Ran, Y., and Zhang, W., "Effect of adhesive and its aging on the performance of piezoelectric sensors in structural health monitoring systems," *Metals* **10**, 1342 (Oct. 2020).

[14] Tanaka, A., Masuda, A., Akahori, S., Higashi, Y., and Miura, N., "A clinging device for structural inspection aerial robot," *The Proceedings of JSME annual Conference on Robotics and Mechatronics (Robomec)* **2018**, 1A1–B11 (12 2018).

[15] Zhu, L., Fu, Y., Chow, R., Spencer, B., Park, J., and Mechitov, K., "Development of a high-sensitivity wireless accelerometer for structural health monitoring," *Sensors* **18**, 262 (jan 2018).

[16] Bedon, C., Bergamo, E., Izzi, M., and Noè, S., "Prototyping and validation of MEMS accelerometers for structural health monitoring—the case study of the pietratagliata cable-stayed bridge," *Journal of Sensor and Actuator Networks* **7**, 30 (jul 2018).

[17] Latt, W. T., Tan, U.-X., Riviere, C. N., and Ang, W. T., "Transfer function compensation in gyroscope-free inertial measurement units for accurate angular motion sensing," *IEEE Sensors Journal* **12**, 1207–1208 (May 2012).

[18] Satme, J., Smith, C., Downey, A. R. J., Bakos, J. D., Vitzilaios, N., and Rizos, D., "Compensation technique for accurate acceleration measurements using a UAV deployable and retrievable sensor package," in [*Sensors and Smart Structures Technologies for Civil, Mechanical, and Aerospace Systems 2022*], Zonta, D., Su, Z., and Glisic, B., eds., SPIE (apr 2022).

[19] Ward, P. and Liu, D., "Design of a high capacity electro permanent magnetic adhesion for climbing robots," in [*2012 IEEE International Conference on Robotics and Biomimetics (ROBIO)*], 217–222 (2012).

[20] Satme, J. N., Yount, R., Vaught, J., Smith, J., and Downey, A. R., "Modal analysis using a uav-deployable wireless sensor network," *Society for Experimental Mechanics, International Modal Analysis Conference* (2023).

[21] Satme, J. and Downey, A., "Drone delivered vibration sensor." GitHub (2022).

[22] Hochreiter, S. and Schmidhuber, J., "Long short-term memory," *Neural Computation* **9**, 1735–1780 (nov 1997).

[23] Gers, F., "Learning to forget: continual prediction with LSTM," in [*9th International Conference on Artificial Neural Networks: ICANN '99*], IEEE (1999).